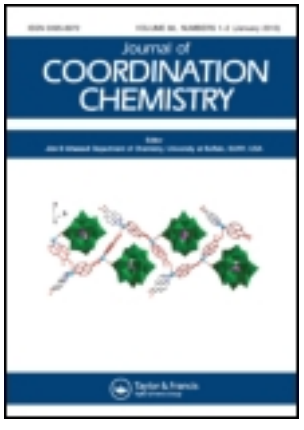

Journal of Coordination Chemistry
Publication details, including instructions for authors and subscription information:
http://www.tandfonline.com/loi/gcoo20

Syntheses, structures, and properties of transition metal complexes with 2-(n-pyridyl)benzimidazole (n = 2, 3, and 4)

Ying-Xia Zhou [a], Xia Li [b], Hai-Yan Zhang [a], Cai-Ling Fan [a], Hong-Yun Zhang [b] & Ben-Lai Wu [a b]

[a] College of Sciences, Henan Agricultural University, Zhengzhou 450002, People's Republic of China

[b] Department of Chemistry, Zhengzhou University, Zhengzhou 450052, People's Republic of China

Published online: 15 Nov 2011.

To cite this article: Ying-Xia Zhou, Xia Li, Hai-Yan Zhang, Cai-Ling Fan, Hong-Yun Zhang & Ben-Lai Wu (2011) Syntheses, structures, and properties of transition metal complexes with 2-(n-pyridyl)benzimidazole (n = 2, 3, and 4), Journal of Coordination Chemistry, 64:23, 4066-4078, DOI: 10.1080/00958972.2011.635375

To link to this article: http://dx.doi.org/10.1080/00958972.2011.635375

Journal of Coordination Chemistry
Vol. 64, No. 23, 10 December 2011, 4066–4078

Syntheses, structures, and properties of transition metal complexes with 2-(*n*-pyridyl)benzimidazole (*n* = 2, 3, and 4)

YING-XIA ZHOU†, XIA LI‡, HAI-YAN ZHANG†, CAI-LING FAN†, HONG-YUN ZHANG*‡ and BEN-LAI WU*‡

†College of Sciences, Henan Agricultural University, Zhengzhou 450002, People's Republic of China
‡Department of Chemistry, Zhengzhou University, Zhengzhou 450052, People's Republic of China

(*Received 29 September 2010; in final form 14 October 2011*)

Three pyridylbenzimidazoles (2-PBIM, 3-PBIM, and 4-PBIM) have been prepared (2-PBIM: 2-(2-pyridyl)-benzimidazole, 3-PBIM: 2-(3-pyridyl)-benzimidazole, 4-PBIM: 2-(4-pyridyl)-benzimidazole). Reactions of several transition metals (Cd^{2+}, Cu^{2+}, Fe^{2+}) with the three ligands gave four new coordination complexes, $[(Cd)_2(2\text{-PBIM})_2(CH_3COO)_4]$ (**1**), $[Cu(3\text{-PBIM})_2(CH_3COO)_2]\cdot 2H_2O$ (**2**), $[Cu(4\text{-PBIM})_2(CH_3COO)_2(H_2O)]\cdot H_2O$ (**3**), and $[Fe(4\text{-PBIM})_2(Cl)_2(H_2O)_2]$ (**4**), respectively. These four complexes have been characterized by X-ray crystallography, IR spectroscopy, and UV absorption spectroscopy. Thermogravimetric properties of **2** and **4** were also measured. X-ray crystallographic studies reveal that these four complexes are very different, although the ligands are similar in structure. The role of hydrogen-bonding and π–π interactions in extending dimensionality of simple complexes has been discussed.

Keywords: Pyridylbenzimidazole; Complex; Crystal structure; Hydrogen bond; π–π Interaction

1. Introduction

Pyridylbenzimidazole has three N-donors and can act as a neutral mono- or bidentate ligand and as an anionic tridentate ligand. Pyridylbenzimidazole has tunable coordination modes and supramolecular interactions because it is a multidentate ligand and includes hydrogen-bonding donor (benzimidazole group) and acceptors (aromatic N atoms) [1]. Therefore, chelate complexes or polymers can be obtained with pyridylbenzimidazoles, and the stability of chelate complexes is much better than that of monodentate complexes. Thus, this type of N-heterocyclic ligand is a good choice in constructing metal-organic frameworks with interesting structures and properties. Many pyridylbenzimidazole complexes have been studied, but most are simple complexes and few polymers are observed [1]. Coordination architectures with pyridylbenzimidazoles as ligands are terminal [2–4] with few examples bridging (scheme 1) [5, 6]. Moreover, this kind of ligand has attracted considerable interest for its

*Corresponding authors. Email: wzhy917@zzu.edu.cn; wbl@zzu.edu.cn

ISSN 0095-8972 print/ISSN 1029-0389 online © 2011 Taylor & Francis
http://dx.doi.org/10.1080/00958972.2011.635375

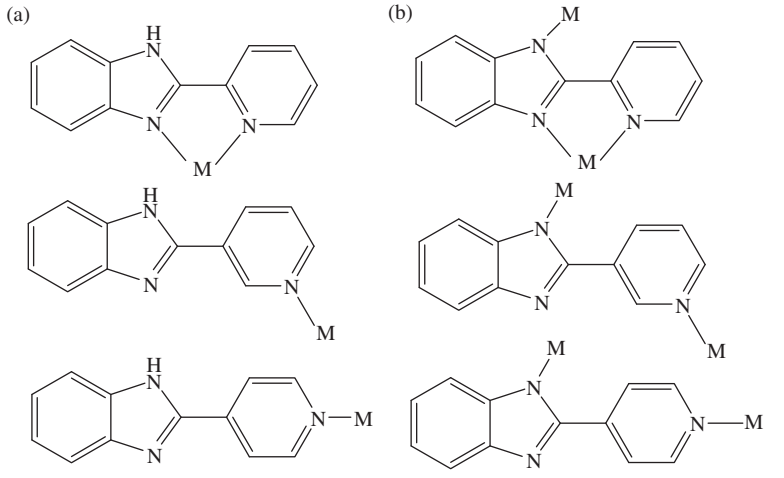

Scheme 1. Coordination mode of pyridylbenzimidazole ligands: (a) chelating-terminal-mode and terminal-mode; (b) chelating-bridging-mode and bridging-mode.

wide-ranging antiviral activities, photochemical and photophysical properties, versatile coordination modes, and potential to form supramolecular aggregates through π–π stacking and hydrogen-bonding [7–16]. To extend the relevant structural types and establish synthetic strategies which could control dimensionality of the complexes, leading to desired organic–inorganic frameworks, we report four transition metal complexes assembled from pyridylbenzimidazoles, 2-(2-pyridyl)-benzimidazole, 2-(3-pyridyl)-benzimidazole, and 2-(4-pyridyl)-benzimidazole. These three ligands coordinate differently and provide low-dimensional building units which further propagate into 3-D supramolecular structures *via* hydrogen bonds, π–π interaction, and other weak intermolecular interactions. In these four complexes, three pyridylbenzimidazoles are terminal [17, 18].

2. Experimental

2.1. *Materials and physical measurements*

All reagents and solvents were reagent grade, purchased from Zhengzhou Huafeng Chemical Reagent Company, and used without purification. Elemental analysis was carried out on a PE 1700 CHN auto elemental analyzer and IR spectra were recorded with an FTS-40 infrared spectrophotometer as KBr pellets from 4000 to 400 cm^{-1}. Ultraviolet absorption spectra were measured using an Agilent 8453 spectrophotometer. Thermal decomposition experiments were carried out by using a Netzsch STA 409 PC/PG instrument from room temperature to about 700°C at a heating rate of 10°C·min^{-1} in air.

Table 1. Crystal data and structure refinement for **1**–**4**.

	1	**2**	**3**	**4**
Empirical formula	$C_{16}H_{15}N_3O_4Cd$	$C_{28}H_{28}N_6O_6Cu$	$C_{28}H_{28}N_6O_6Cu$	$C_{24}H_{22}Cl_2N_6O_2Fe$
Formula weight	425.71	608.14	608.10	553.23
Temperature (K)	293(2)	291(2)	291(2)	291(2)
Wavelength (Å)	0.71073	0.71073	0.71073	0.71073
Crystal system	Monoclinic	Monoclinic	Triclinic	Triclinic
Space group	*P2(1)/c*	*P2(1)/c*	$P\bar{1}$	$P\bar{1}$
Unit cell dimensions (Å, °)				
a	9.8337(7)	8.879(16)	7.787(16)	7.019(6)
b	21.4801(15)	9.2105(16)	12.77(3)	9.215(7)
c	7.92 57(6)	18.354(3)	14.46(3)	9.360(8)
α	90.0	90.0	83.62(3)	76.127(9)
β	108.0690(10)	99.969(2)	77.33(3)	74.557(9)
γ	90.0	90.0	82.85(3)	86.709(9)
Volume (Å^3), *Z*	1591.6(2), 4	1478.4(4), 2	1387(5), 2	566.5(8), 1
Calculated density (Mg m^{-3})	1.777	1.447	1.456	1.622
Absorption coefficient (mm^{-1})	1.398	0.798	0.841	0.939
F(000)	848	670	630	284
Crystal size (mm^3)	0.18 × 0.11 × 0.09	0.18 × 0.17 × 0.14	0.26 × 0.19 × 0.11	0.19 × 0.09 × 0.08
θ range for data collection (°)	2.38–27.50	2.33–25.50	2.70–25.50	2.32–27.49
Limiting indices	$-12 \le h \le 5$; $-27 \le k \le 27$; $-10 \le l \le 9$	$-10 \le h \le 10$; $-11 \le k \le 7$; $-22 \le l \le 21$	$-9 \le h \le 9$; $-15 \le k \le 15$; $-17 \le l \le 17$	$-9 \le h \le 9$; $-11 \le k \le 11$; $-12 \le l \le 12$
Reflections collected/unique	9591/3645 [*R*(int) = 0.0251]	8062/2689 [*R*(int) = 0.0391]	10,250/5114 [*R*(int) = 0.0333]	4927/2522 [*R*(int) = 0.0275]
Data/restraints/parameters	3645/0/219	2689/6/197	5114/0/380	2522/3/160
Goodness-of-fit on F^2	1.021	1.036	1.059	1.016
R_1	0.0253	0.0548	0.0499	0.0444
wR_2	0.0578	0.1723	0.1341	0.1039
$\Delta\rho_{min}$ and $\Delta\rho_{max}$ (e Å^{-3})	0.414 and −0.475	0.382 and −0.304	0.324 and −0.737	0.463 and −0.426

2.2. *X-ray crystallography*

Suitable single crystals of **1**–**4** were chosen for data collection. Crystal data collection was performed using graphite monochromated Mo-Kα (λ = 0.071073 nm) radiation on a Rigaku Raxis-IV X-ray diffractometer at 293(2) K for **1** and 291(2) K for **2**, **3**, and **4**. The structures were solved by direct methods with SHELXS-97 and refined on F^2 by full-matrix least-squares using SHELXL-97 program package [19]. All non-hydrogen atoms were refined anisotropically, and hydrogen atoms were located and included at their calculated positions. Details of the crystal structure determinations and structure refinement for **1**–**4** are summarized in table 1, and selected bond lengths and angles are listed in tables 2 and 3, respectively. Full atomic data are available as a file in crystallographic information file (CIF) format.

2.3. *Syntheses of 2-PBIM, 3-PBIM, and 4-PBIM*

2-PBIM was synthesized following a modified literature method [20, 21] and the synthesis procedure was modified. 2-Pyridinecarboxylic acid (60 mmol), PPA (polyphosphoric acid) (25 g), and glycol (70 mL) were added to a four-necked round-bottomed flask (250 mL) with a reflux condenser. Then, the mixture was heated and *o*-phenylenediamine (60 mmol) was added to the flask with vigorous stirring at 80°C.

Table 2. Selected bond distances (Å) for **1**–**4**.

1		2		3		4	
Cd(1)–N(2)	2.3116(19)	Cu(1)–O(4)	1.937(3)	Cu(1)–O(3)	1.937(4)	Fe(1)–O(1A)	2.159(2)
Cd(1)–O(1A)	2.3611(17)	Cu(1)–N(1)	2.041(4)	Cu(1)–N(4)	2.024(5)	Fe(1)–N(1)	2.216(3)
Cd(1)–O(3)	2.463(2)	Cu(1)–O(4A)	1.937(3)	Cu(1)–O(2)	1.936(4)	Fe(1)–Cl(1)	2.5503(15)
Cd(1)–O(2)	2.5497(18)	Cu(1)–N(1A)	2.041(4)	Cu(1)–N(3)	2.035(5)	Fe(1)–O(1)	2.159(2)
Cd(1)–O(4)	2.293(2)	O(1)–H(2W)	0.8621	Cu(1)–O(5)	2.262(4)	Fe(1)–N(1A)	2.216(3)
Cd(1)–N(1)	2.403(2)	O(2)–H(3W)	0.8381	O(1)–C(26)	1.240(4)	Fe(1)–Cl(1A)	2.5502(15)
Cd(1)–O(1)	2.4063(19)	O(3)–C(1)	1.221(7)	O(2)–C(26)	1.277(5)	O(1)–H(1W)	0.8261
O(1)–C(13)	1.264(3)	N(1)–C(7)	1.328(5)	O(4)–C(28)	1.247(5)	N(1)–C(11)	1.345(4)
O(2)–C(13)	1.245(3)	N(1)–C(3)	1.341(6)	O(5)–H(2W)	0.8291	N(2)–C(7)	1.334(3)
O(3)–C(15)	1.244(4)	N(2)–C(8)	1.362(5)	O(6)–H(3W)	0.8875	N(2)–C(1)	1.398(4)
O(4)–C(15)	1.260(3)	N(2)–C(9)	1.385(6)	O(6)–H(4W)	0.8408	N(3)–C(7)	1.370(4)
N(1)–C(1)	1.337(3)	N(2)–H(2)	0.8600	N(1)–C(6)	1.356(5)	N(3)–C(6)	1.377(3)
N(1)–C(5)	1.350(3)	N(3)–C(8)	1.299(6)	N(1)–C(7)	1.367(5)	N(3)–H(3N)	0.8600
N(2)–C(6)	1.319(3)	N(3)–C(10)	1.409(5)	N(1)–H(1N)	0.890(4)		
N(2)–C(7)	1.385(3)			N(2)–C(6)	1.323(5)		
N(3)–C(6)	1.358(3)			N(2)–C(8)	1.387(5)		
N(3)–C(12)	1.385(3)						

The mixed solution was kept stirring at 180–200°C for 4 h, turning deep green. The mixture was cooled, 100 mL of H_2O added to the reaction solution at 100°C, and the pH of the solution adjusted to about 7.0 with aqueous solution of Na_2CO_3. Gray-green precipitate appeared, was collected by filtration, and recrystallized with 95% ethanol, giving gray needle-like crystals of 2-PBIM with 36.2% yield based on *o*-phenylenediamine. M.p.: 222–224°C. Elemental Anal. (%): C, 73.75; H, 4.55; N, 21.36 (Calcd (%): C, 73.83; H, 4.65; N, 21.52). IR (KBr, cm^{-1}): 3065(m), 2872(m), 1587(s), 1457(m), 1385(s), 1144(m), 750(s), 696(s).

The synthesis procedure of 3-PBIM and 4-PBIM is similar to that of 2-PBIM. Yellow needle-like crystals of 3-PBIM (1.5 g) were obtained. Yield based on *o*-phenylenediamine was 39.5%. M.p.: 216–218°C. Elemental Anal. (%): C, 73.72; H, 4.56; N, 21.38 (Calcd (%): C, 73.83; H, 4.65; N, 21.52). IR (KBr, cm^{-1}): 3051(m), 1625(m), 1581(m), 1442(s), 1317(m), 1278(m), 1117(m), 815(m), 744(s), 705(m). Yellow needle-like crystals of 4-PBIM (1.6 g) were obtained. Yield based on *o*-phenylenediamine was 53.0%. M.p.: 219–222°C. Elemental Anal. (%): C, 74.03; H, 4.52; N, 21.29 (Calcd (%): C, 73.83; H, 4.65; N, 21.52). IR (KBr, cm^{-1}): 3055(w), 1609(s), 1536(w), 1434(s), 1317(m), 1282(m), 1234(m), 1001(s), 839(m), 745(s), 693(m).

2.4. *Syntheses of 1–4*

2.4.1. [$(Cd)_2$(2-PBIM)$_2$$(CH_3COO)_4$] (1). Solution of $Cd(CH_3COO)_2 \cdot 2H_2O$ (0.27 g, 1.0 mmol) in DMF (10 mL) was added dropwise to a solution of 2-PBIM (0.2 g, 1.0 mmol) dissolved in water (10 mL) while vigorously stirring, and the mixed solution was continuously stirred for 20 min, then sealed in a 15 mL Teflon-lined steel reactor. The steel reactor was heated in an oven at 140°C for 72 h, then cooled to room temperature at a rate of $10°C \cdot h^{-1}$. The mixed solution was filtered and the filtrate was allowed to evaporate at room temperature. Colorless block crystals of **1** suitable for

Table 3. Selected bond angles (°) for **1**–**4**.

1		**2**	
O(4)–Cd(1)–N(2)	98.75(7)	O(4A)–Cu(1)–O(4)	180.0(3)
O(4)–Cd(1)–O(1A)	104.29(7)	O(4A)–Cu(1)–N(1)	89.55(14)
N(2)–Cd(1)–O(1A)	143.32(7)	O(4)–Cu(1)–N(1)	90.45(14)
O(4)–Cd(1)–N(1)	169.81(7)	N(1)–Cu(1)–N(1A)	180.000(1)
N(2)–Cd(1)–N(1)	71.16(7)	H(1W)–O(1)–H(2W)	119.2
O(1A)–Cd(1)–N(1)	83.94(7)	H(3W)–O(2)–H(4W)	110.4
O(4)–Cd(1)–O(1)	90.49(7)	C(1)–O(4)–Cu(1)	124.3(4)
N(2)–Cd(1)–O(1)	135.76(7)	C(7)–N(1)–C(3)	117.8(4)
O(1A)–Cd(1)–O(1)	72.65(8)	C(7)–N(1)–Cu(1)	120.2(3)
N(1)–Cd(1)–O(1)	97.80(7)	C(3)–N(1)–Cu(1)	122.0(3)
O(4)–Cd(1)–O(3)	54.87(7)	C(8)–N(2)–C(9)	105.7(4)
N(2)–Cd(1)–O(3)	84.57(7)	C(8)–N(2)–H(2)	127.1
O(1A)–Cd(1)–O(3)	85.81(6)	C(9)–N(2)–H(2)	127.1
N(1)–Cd(1)–O(3)	120.96(7)	C(8)–N(3)–C(10)	105.1(4)
O(4)–Cd(1)–O(2)	99.70(7)		
N(2)–Cd(1)–O(2)	84.11(6)		
O(1A)–Cd(1)–O(2)	118.88(6)		
N(1)–Cd(1)–O(2)	81.06(6)		
O(1)–Cd(1)–O(2)	51.66(6)		
O(3)–Cd(1)–O(2)	149.95(6)		
3		**4**	
O(2)–Cu(1)–O(3)	179.28(10)	O(1)–Fe(1)–O(1A)	179.999(2)
O(2)–Cu(1)–N(4)	88.04(12)	O(1)–Fe(1)–N(1)	91.60(9)
O(3)–Cu(1)–N(4)	91.55(12)	O(1)–Fe(1)–N(1A)	88.40(9)
O(2)–Cu(1)–N(3)	88.64(13)	N(1)–Fe(1)–N(1A)	180.00(12)
O(3)–Cu(1)–N(3)	91.64(13)	N(1)–Fe(1)–Cl(1A)	89.63(8)
N(4)–Cu(1)–N(3)	168.03(12)	O(1)–Fe(1)–Cl(1)	86.00(8)
O(2)–Cu(1)–O(5)	89.92(19)	O(1A)–Fe(1)–Cl(1)	94.00(8)
O(3)–Cu(1)–O(5)	90.72(19)	N(1)–Fe(1)–Cl(1)	90.37(8)
N(4)–Cu(1)–O(5)	97.18(11)	Cl(1A)–Fe(1)–Cl(1)	180.0
N(3)–Cu(1)–O(5)	94.31(12)		
C(26)–O(2)–Cu(1)	123.1(3)		
C(28)–O(3)–Cu(1)	125.6(3)		
Cu(1)–O(5)–H(1W)	116.9		
Cu(1)–O(5)–H(2W)	130.3		
H(1W)–O(5)–H(2W)	110.2		
H(3W)–O(6)–H(4W)	110.1		

Symmetry transformations used to generate equivalent atoms: A $-x+1, -y+1, -z+1$ for **1** and **2**; A $-x, -y+2, -z+2$ for **4**.

single-crystal X-ray diffraction analysis were obtained after 3 days with 23% yield based on 2-PBIM. IR (cm^{-1}, KBr): 3002(w), 2872(m), 1557(s), 1529(m), 1436(s), 1420(s), 1157(m), 1013(m), 750(s), 670(s).

2.4.2. $[Cu(3\text{-}PBIM)_2(CH_3COO)_2]\cdot 2H_2O$ (2). A solution of $Cu(CH_3COO)_2\cdot H_2O$ (0.06 g, 0.3 mmol) in methanol (10 mL) was added dropwise to a solution of 3-PBIM (0.06 g, 0.3 mmol) dissolved in ethanol (10 mL) with stirring at room temperature for 60 min; a little blue precipitate appeared after 30 min. The mixture was filtered and the filtrate was allowed to evaporate at room temperature. Blue block single crystals of **2** were obtained after about 30 days, filtered, washed with a small amount of methanol,

and air-dried. Yield 0.13 g (46%) based on 3-PBIM. IR (KBr, cm^{-1}): 2926(w), 1565(s), 1446(s), 1407(s), 1319(w), 1195(m), 1011(w), 818(m), 749(m), 697(m).

2.4.3. $[Cu(4\text{-}PBIM)_2(CH_3COO)_2(H_2O)]\cdot H_2O$ (3) and $[Fe(4\text{-}PBIM)_2(Cl)_2(H_2O)_2]$ (4). The syntheses of **3** and **4** are similar to that of **2**. Blue block crystals for **3** and yellow acerose crystals for **4** were obtained with 42% yield for **3** and 51% yield for **4** based on 4-PBIM. IR for **3** (KBr, cm^{-1}): 3060(w), 1618(s), 1562(s), 1533(m), 1433(s), 1412(m), 1318(s), 1116(w), 1025(m), 814(m), 743(s). IR for **4** (KBr, cm^{-1}): 3097(w), 1614(s), 1542(w), 1498(w), 1430(m), 1317(m), 1234(m), 1114(w), 1014(m), 835(m), 745(s), 700(w).

3. Results and discussion

3.1. *Crystal structures of 1–4*

3.1.1. $[(Cd)_2(2\text{-}PBIM)_2(CH_3COO)_4]$ (1). Crystal structure parameters, selected bond lengths, and angles of **1** are listed in tables 1–3, respectively. The coordination geometry and atom labeling in the crystal structure of **1** are shown in figure 1. Complex **1** is binuclear, $[(Cd)_2(2\text{-}PBIM)_2(CH_3COO)_4]$, with two equivalent structural units corresponding to one-half of the dimer. In **1**, the coordination environment of two symmetrical Cd^{2+} is the same, and two Cd^{2+} are bridged by two CH_3COO^- with each Cd^{2+} seven-coordinate with five oxygen atoms from three CH_3COO^- and two nitrogen atoms from one 2-PBIM. The coordination sphere around Cd^{2+} can be described as a distorted pentagonal bipyramid. Acetate is flexible and can possess many coordination modes, roughly classified into five types: monodentate, bidentate-chelating, bidentate-bridging, tridentate-bridging-chelating, and tetradentate-bridging-chelating [22, 23]. In **1**, CH_3COO^- is tridentate-bridging-chelating with two Cd^{2+} ions connected into a dimeric structure by two tridentate carboxylates and bidentate-chelating with two oxygen atoms of a carboxylate coordinated to the same Cd^{2+}. In **1**, the dimeric structure is constrained by a crystallographic centre of inversion that lies at the centre of the Cd_2O_2 core and the quadrilateral Cd(1)O(1)Cd(1A)O(1A) is a parallelogram. In **1**, two 2-PBIM are chelating terminal, forming two five-membered chelate rings. The chelating mode of 2-PBIM results from suitable location of two nitrogen atoms, in contrast to 3-PBIM (in **2**) and 4-PBIM (in **3** and **4**) where the chelate ring formation is impossible.

In the crystal structure of **1**, there is one hydrogen bond (table 4), the intermolecular hydrogen bond of the non-coordinating N–H group from imidazole ring and oxygen of chelated carboxyl from adjacent structural units, $N(3)\text{–}H(1')\cdots O(2B) = 2.724(3)$ Å. The structural units are linked into a 1-D chain by this intermolecular hydrogen, and the 1-D chains are stacked in parallel.

In **1**, 2-PBIM is almost in a plane with face-to-face distances between pyridine rings and benzene rings of neighboring units of 3.7087(2) Å, indicating π–π stacking interactions. Another kind of π–π stacking interactions exist inter-chain; the face-to-face distances between pyridine rings of 2-PBIM in adjacent chains are

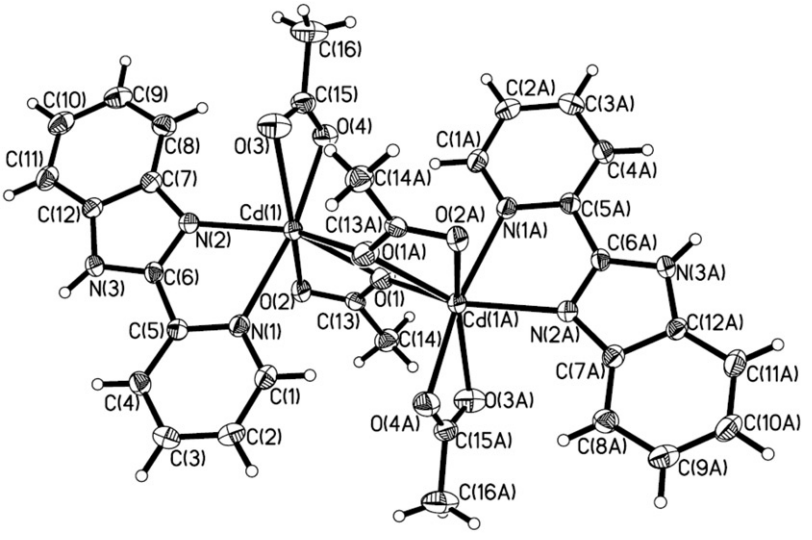

Figure 1. The molecular structure of **1**.

Table 4. Hydrogen-bond distances for **1**–**4** (Å)

D–H···A	*d*(D···A)	D–H···A	*d*(D···A)
Complex **1**		Complex **3**	
N(3)–H(1′)···O(2B)	2.724(3)	O(6)–H(4W)···O(4)	2.889(7)
Complex **2**		O(5)–H(2W)···N(2A)	2.864(7)
N(2)–H(2)···O(1B)	2.793(5)	O(5)–H(1W)···O(1B)	2.766(7)
O(2)–H(4W)···O(1A)	2.763(6)	N(6)–H(6N)···O(1C)	2.789(7)
O(2)–H(3W)···N(3A)	2.735(6)	N(1)–H(1N)···O(4D)	2.836(7)
O(1)–H(2W)···O(3)	2.542(7)	Complex **4**	
O(1)–H(1W)···N(2C)	2.793(5)	O(1)–H(2W)···Cl(1B)	3.571(4)
		O(1)–H(1W)···N(2C)	2.812(3)
		N(3)–H(3N)···Cl(1D)	3.196(3)

Symmetry transformations used to generate equivalent atoms: A $-x+1, -y+1, -z+1$; B $-x, -y+1, -z$ (for **1**), A $-x+1, -y+1, -z+1$; B $x+1, y, z$; C $x-1, y, z$ (for **2**), A $-x+1, -y+2, -z+2$; B $x+1, y, z$; C $-x+1, -y+2, -z+1$; D $-x+1, -y+1, -z+2$ (for **3**), A $-x, -y+2, -z+2$; B $-x+1, -y+2, -z+2$; C $x, y+1, z$; D $x, y, z-1$ (for **4**).

3.5071(2) Å. These π–π stacking interactions and the intermolecular hydrogen bond mentioned above play an important role in the 3-D supramolecular structures of **1**.

3.1.2. $[Cu(3\text{-PBIM})_2(CH_3COO)_2]\cdot 2H_2O$ (2). Complex **2** is obtained by reaction of 3-PBIM and $Cu(CH_3COO)_2\cdot H_2O$ in methanol; **2** is a discrete monomer. The structure consists of one Cu(II) cation, two 3-PBIM, two CH_3COO^-, and two lattice water molecules, as shown in figure 2. Complex **2** has Cu(II)N_2O_2 configuration with approximate diamond-shaped quadrilateral geometry with Cu(1)–O(4A) = Cu(1)–O(4) = 1.937(3) Å and Cu(1)–N(1) = Cu(1)–N(1A) = 2.041(4) Å (listed in table 2), two nitrogen atoms from 3-PBIM and two oxygen atoms from CH_3COO^- located at the

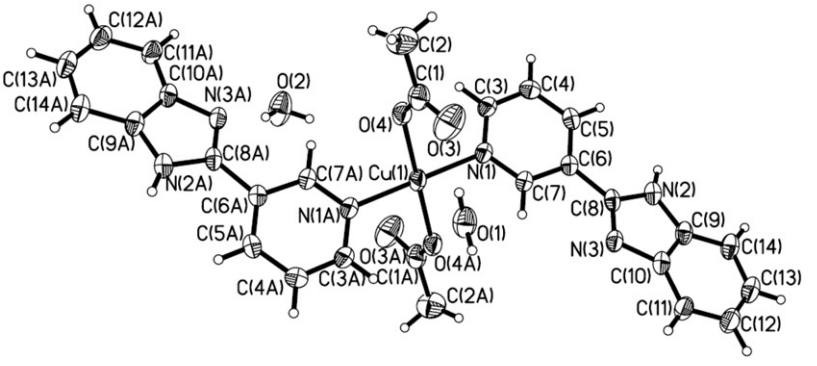

Figure 2. The molecular structure of **2**.

four corners of quadrilateral, two H_2O molecules do not participate in coordination. In **2**, CH_3COO^- is monodentate with *trans*-conformations and two 3-PBIM are terminal because it is impossible for 3-PBIM to form a chelate ring.

Lattice water molecules are connected with uncoordinated nitrogen atoms (from imine and amidogen) of 3-PBIM and oxygen atoms of coordinated CH_3COO^- to form a complicated hydrogen-bonding network (table 4). As a result, the structural units of **2** extend into a 2-D supramolecular framework, and the 2-D networks extend to a 3-D supramolecule by other weaker interactions.

3.1.3. $[Cu(4\text{-PBIM})_2(CH_3COO)_2(H_2O)]\cdot H_2O$ (3). The structure unit of **3** is shown in figure 3. Cu^{2+} is five-coordinate by three oxygen atoms from two CH_3COO^- and one coordinated water and two nitrogen atoms of 4-PBIM, forming a distorted tetragonal pyramid; another water molecule does not participate in coordination. In **3**, pyridine rings and imidazole rings of 4-PBIM are not coplanar, with dihedral angle of 2.7° for rings C(1)C(2)C(3)C(4)C(5)N(3) and N(1)C(6)N(2)C(7)C(8), and 11.3° for rings C(13)C(14)C(15)C(16)C(17)N(4) and N(5)C(18)N(6)C(19)C(20). The different angles between pyridine and imidazole are perhaps because formation of different hydrogen bonds of N(1), N(2), N(5) and N(6) lead to distortion of 4-PBIM. The two coordinated CH_3COO^- anions are monodentate and *cis*, different from the *trans*-geometry in **2**. 4-PBIM in **3** are terminal, similar to 3-PBIM in **2**.

In the crystal structure of **3**, there are five types of hydrogen bonds (table 4). Coordination water and lattice water with the uncoordinated oxygen of the carboxyl and nitrogen (from imine or amidogen) form a complicated hydrogen-bonding network. The units of **3** extended into a 3-D supramolecule by this hydrogen bond network.

3.1.4. $[Fe(4\text{-PBIM})_2(Cl)_2(H_2O)_2]$ (4). Complex **4** is also a simple complex, similar to **2** and **3**. As shown in figure 4, each Fe(II) is six-coordinate by two nitrogen atoms of pyridine from the two 4-PBIM, two Cl^-, and two oxygen atoms of coordinated water. The coordination geometry of Fe(II) can be described as an elongated octahedron. Two 4-PBIM coordinate terminal to one Fe(II) through pyridine as they do in **3**. In **4**, pyridine rings and imidazole rings from 4-PBIM are not coplanar, with dihedral angle of 2.8°. The molecular structure of **4** is similar to the Zn(II) complex [24].

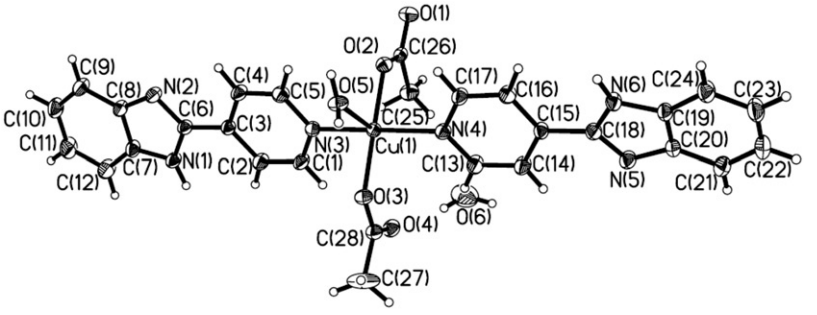

Figure 3. The molecular structure of **3**.

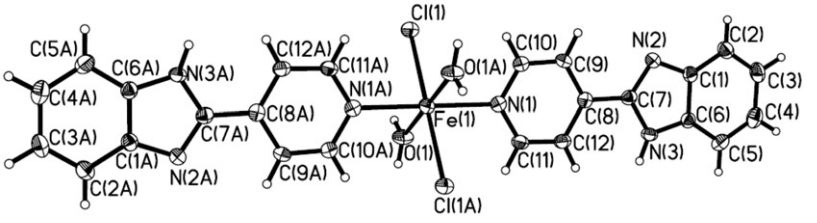

Figure 4. Structure unit drawing of **4**.

Hydrogen bonds exist in **4**, too (table 4). Coordinated water with imine of 4-PBIM from neighboring units form hydrogen bonds O(1)–H(1W)···N(2C) of 2.812(3) Å, the amidogen N of imidazole from 4-PBIM with Cl^- of neighboring units form weak hydrogen bonds, N(3)–H(3N)···Cl(1D) of 3.196(3) Å, and coordinated water with Cl^- of adjacent units form another weaker hydrogen bond, O(1)–H(2W)···Cl(1B) of 3.571(4) Å. The lattice construction of **4** can be presented in three stages: the shortest hydrogen bond (2.812 Å) links complex molecules into a ribbon expanding along the *b*-axis, another hydrogen bond (3.196(3) Å) joins the ribbons into a plane parallel to (1 0 0), and the last hydrogen bond (3.571(4) Å) connects the planes into a 3-D structure. π–π stacking interactions are also observed with centroid-to-centroid distance of 3.5 Å and the deviation angle of 2.7° between pyridyl and benzene rings of neighbouring units, indicating weak twofold π–π interactions, and the weak π–π stacking interactions made the 2-D frameworks more stable.

As described above, all four complexes are discrete simple complexes and the pyridylbenzimidazole ligands are terminal. Each crystal is a supermolecule [24–29] and the crystal-packing mode of **1**–**4** has been analyzed with construction strongly depending on hydrogen bonds, π–π interactions, and other weaker intermolecule interactions. Hydrogen bonds are the main forces holding subunits together and sustaining the crystal framework, while π–π interactions play important roles to direct the stacking fashion [24].

3.2. *UV spectra analysis of 1–4*

UV absorption spectra for 2-PBIM, 3-PBIM, 4-PBIM, and **1**–**4** (10^{-5}–10^{-6} mol·L^{-1} in methanol) are shown in figures 5 and 6. They all exhibit absorptions from 200 to 400 nm

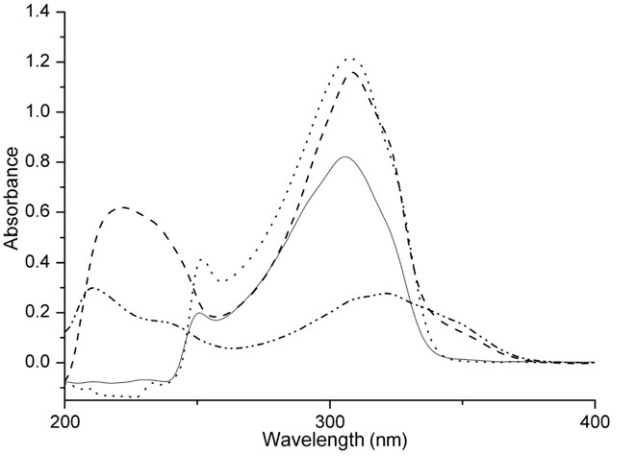

Figure 5. UV absorption spectra of 2-PBIM, 3-PBIM, **1** and **2** in methanol (10^{-5}–10^{-6} mol · L^{-1}; dashed line, 2-PBIM; dash-dotted line, **1**; solid line, 3-PBIM; dotted line, **2**).

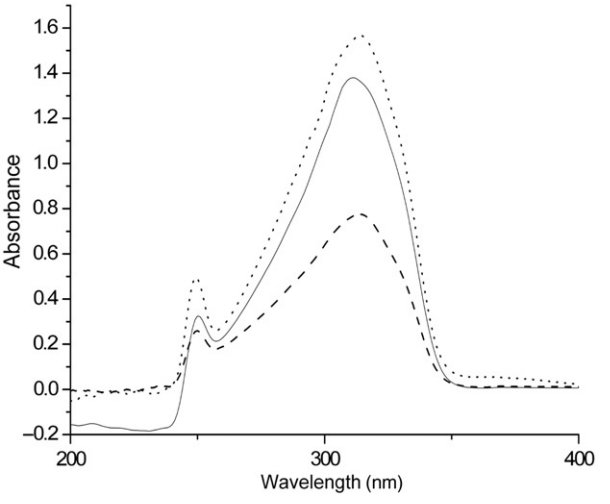

Figure 6. UV absorption spectra of 4-PBIM, **3** and **4** in methanol (10^{-5}–10^{-6} mol · L^{-1}; solid line, 4-PBIM; dashed line, **3**; dotted line, **4**).

with maximum absorptions at 225, 250, and 310 nm, respectively, attributed to $n \rightarrow \pi^*$ and $\pi \rightarrow \pi^*$ transitions of pyridine and benzene. Compared with the free ligands, the absorption bands of **1**–**4** are red-shifted (figures 5 and 6). The conjugated system is expanded due to coordination of metal, leading to energy reduction for $n \rightarrow \pi^*$ and $\pi \rightarrow \pi^*$ transitions [30]. Thus, displacement of electron clouds from pyridine or benzene rings to metal ions occur, causing red shift of $n \rightarrow \pi^*$ and $\pi \rightarrow \pi^*$ transition.

3.3. *Thermogravimetric analysis of 2 and 4*

Thermogravimetric (TG) analysis in air with a heating rate of 10°C·min^{-1} was performed on polycrystalline samples for **2** and **4** (figures 7 and 8).

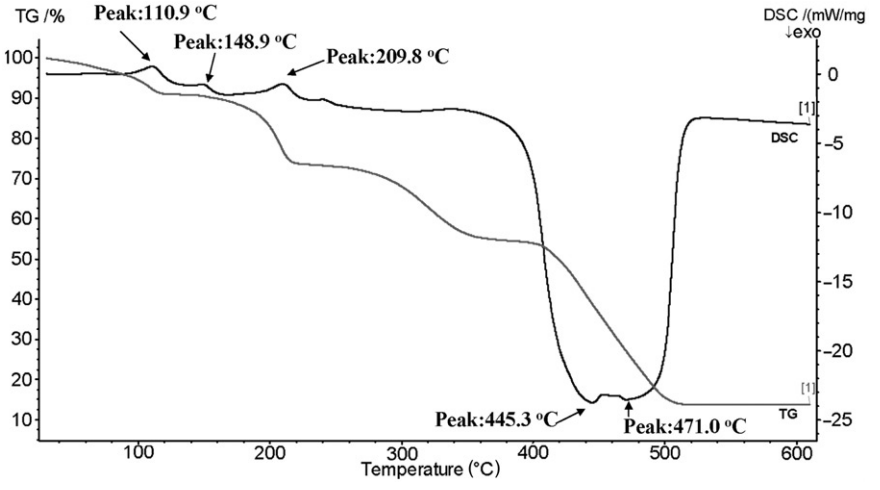

Figure 7. TG-DSC curves of **2**.

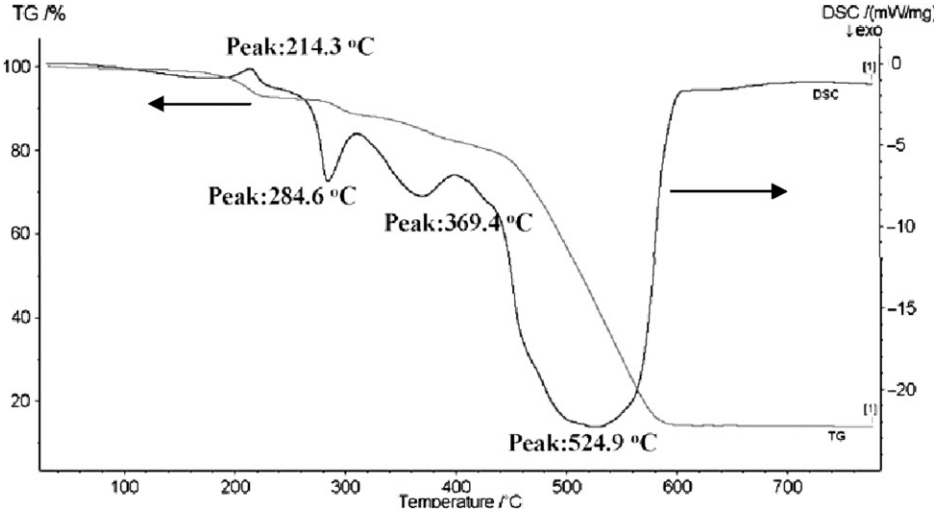

Figure 8. TG-DSC curves of **4**.

For **2**, the weight loss of 7.2% before 130°C is equivalent to loss of two lattice water molecules per formula unit (Calcd: 5.9%). Two major weight losses occur after 200°C. The first from 130°C to 250°C with DSC peak at 209.8°C is due to loss of two coordinated CH_3COO^- (calculated mass loss of 19.4% observed, 18.1%). The next transition from 250°C to 530°C is a consecutive complicated process containing two contiguous DSC peaks at 445.3°C and 471.0°C. This thermal event is due to decomposition of two 3-PBIM molecules and is accompanied by the formation of CuO. The process at 400–530°C is related to gradual elimination of carbon resulting from decomposition in air [31]. The total mass loss to 600°C is 86.25%, which agrees with the theoretical value (87.0%) calculated by taking CuO as the final products.

As shown in figures 7 and 8, **4** is more stable than **2**. Four transitions appear in the decomposition process of **4**. The first transition ranging from 200°C to 240°C is loss of 6.9%, related to loss of two coordinated water molecules (Calcd: 6.5%). The second transition ranging from 280°C to 340°C is a loss of 6.1%, related to loss of one Cl^- (Calcd: 6.4%). The third transition ranging from 340°C to 420°C is loss of 6.2% from another Cl^- (Calcd: 6.4%). The last transition of 420°C to 600°C is two 4-PBIM molecules. The calculated mass loss of 70.6% for the fourth thermal event agrees with that on TG curve (68.5%). The decomposition residue of **4** is 13.8% revealed by the TG curve, which should be FeO (Calcd: 13.0%).

4. Conclusions

2-PBIM coordinates terminal-chelating to Cd(II) and 3-PBIM and 4-PBIM coordinate terminal. The three isomeric ligands (2-PBIM, 3-PBIM and 4-PBIM) coordinate terminal with metal ions.

Different coordination environments around the metal ions offer distinctive supramolecular interaction sites for each structural unit. The complex units were connected by hydrogen-bonding, π–π interactions, and other weaker intermolecule interactions, with hydrogen bonds the main forces holding the subunits together, while π–π interactions normally play important roles to direct the stacking.

Supplementary material

The supplementary crystallographic data for the structural analyses of this article have been deposited *via* the Cambridge Crystallographic Data Centre, CCDC Reference Nos.: 607529 (for **1**), 635053 (for **2**), 635051 (for **3**) and 635052 (for **4**). Copies of these can be obtained free of charge from: The Director, CCDC, 12 Union Road, Cambridge CB2 1EZ, UK (Fax: +44-1223-336-033; Email: deposit@ccdc.cam.ac.uk or www: http://www.ccdc.cam.ac.uk/data_request/cif).

Acknowledgments

We gratefully acknowledge financial support from the National Natural Science Foundation of China (20771094, 20671083) and the Science and Technology Key Task of Henan Province (0524270061).

References

[1] Y. Yang, M.H. Zeng, X.H. Zhao, H. Liang. *Inorg. Chim. Acta*, **362**, 3065 (2009).
[2] S.M. Yue, H.B. Xu, J.F. Ma, Z.M. Su, Y.H. Kan, H.J. Zhang. *Polyhedron*, **25**, 635 (2006).
[3] B.C. Dave, R.S. Czernuszewicz. *Inorg. Chim. Acta*, **227**, 33 (1994).

[4] V. Tangoulis, D.A. Malamatari, K. Soulti, V. Stergiou, C.P. Raptopoulou, A. Terzis, T.A. Kabanos, D.P. Kessissoglou. *Inorg. Chem.*, **35**, 4974 (1996).
[5] M.H. Zeng, X.C. Shen, S.W. Ng. *Acta Crystallogr., Sect. E*, **62**, 2194 (2006).
[6] J.H. Liu, X.Y. Wu, Q.Z. Zhang, X. He, C.Z. Lu. *Chinese J. Struct. Chem.*, **25**, 1507 (2006).
[7] J.G. Lambardino, E.H. Wiseman. *J. Med. Chem.*, **17**, 1182 (1974).
[8] V.G. Vaidyanathan, B.U. Nair. *J. Inorg. Biochem.*, **91**, 405 (2002).
[9] V.G. Vaidyanathan, B.U. Nair. *J. Inorg. Biochem.*, **94**, 121 (2003).
[10] R.B. Martin, H. Sigel (Eds.). *Metal Ions in Biological Systems*, Vol. 9, Chap. 1, p. 1, Marcel Dekker, New York (1979).
[11] R.R. Tidwell, S.K. Jones, N.A. Naiman, L.C. Berger, W.B. Brake, C.C. Dykstra, J.E. Hall. *Antimicrob. Agents Chemother.*, **37**, 1713 (1993).
[12] S. Santra, S.K. Dogra. *J. Mol. Struct.*, **476**, 223 (1999).
[13] C.Y. Su, B.S. Kang, Q.C. Yang, T.C.W. Mak. *J. Chem. Soc., Dalton Trans.*, 1857 (2000).
[14] C.J. Matthews, V. Broughton, G. Bernardinelli, X. Melich, G. Brand, A.C. Willis, A.F. Williams. *New J. Chem.*, **27**, 354 (2003).
[15] D. Moon, M.S. Lah, R.E.D. Sesto, J.S. Miller. *Inorg. Chem.*, **41**, 4708 (2002).
[16] B.S. Hammes, M.T. Kieber-Emmons, R. Sommer, A.L. Rheingold. *Inorg. Chem.*, **41**, 1351 (2002).
[17] C.J. Matthews, W. Clegg, S.L. Heath, N.C. Martin, M.N.S. Hill, J.C. Lockhart. *Inorg. Chem.*, **37**, 199 (1998).
[18] M. Vaidyanathan, R. Balamurugan, U. Sivagnaram, M. Palaniandavar. *J. Chem. Soc., Dalton Trans.*, 3498 (2001).
[19] G.M. Sheldrick. *SHELXS-97 and SHELXL-97. Program for Crystal Structure Solution and Refinement*, University of Göttingen, Germany (1997).
[20] L.F. Jin, F.P. Xiao, X.W. Chen. *Chem. Reag.*, **25**, 233 (2003) (in Chinese).
[21] L.G. Wang, Z.Y. Wang, S.G. Liu. *Fine Chemical*, **19**, 257 (2002) (in Chinese).
[22] X.M. Chen, M.L. Tong. *University Chemistry*, **12**, 24 (1997) (in Chinese).
[23] J.F. Ma, J.J. Ni. *Prog. Chem.*, **8**, 259 (1996) (in Chinese).
[24] X.P. Li, M. Pan, S.R. Zheng, Y.R. Liu, Q.T. He, B.S. Kang, C.Y. Su. *Cryst. Growth Des.*, **7**, 2481 (2007).
[25] G.R. Desiraju. *Perspectives in Supramolecular Chemistry: The Crystal as a Supramolecular Entity*, Wiley, Chichester (1996).
[26] D. Braga. *J. Chem. Soc., Dalton Trans.*, **21**, 3705 (2000).
[27] B. Moulton, M. Zaworotko. *J. Chem. Rev.*, **101**, 1629 (2001).
[28] A.M. Beatty. *Cryst. Eng. Commun.*, **51**, 1 (2001).
[29] A.J. Blake, N.R. Champness, P. Hubberstey, W.S. Li, M.A. Withersby, M. Schröder. *Coord. Chem. Rev.*, **183**, 117 (1999).
[30] H.X. Wu, Z.M. Wang, H.F. Yang, X.B. Yu. *J. Chinese Rare Earth Soc.*, **20**, 289 (2002) (in Chinese).
[31] X.Q. Shen, H.J. Zhong, H. Zheng, H.Y. Zhang, G.H. Zhao, Q.A. Wu, H.Y. Mao, E.B. Wang, Y. Zhu. *Polyhedron*, **23**, 1851 (2004).